# The maternal vGluT2 and embryonic mGluR3 signaling relay system controls offspring wing dimorphism in pea aphid

Yiyang Yuan[1], Yanyan Wang[2,3], Wanwan Ye[2,3], Liqiang Xie[2,4], Erliang Yuan[2], Huijuan Guo[2], Shifan Wang[5], Fang Dong[6], Keyan Zhu-Salzman[7], Feng Ge[1]*, Yucheng Sun[2]*

[1]Institute of Plant Protection, Shandong Academy of Agricultural Sciences, Jinan 250100, Shandong Province, China.

[2]State Key Laboratory of Integrated Management of Pest Insects and Rodents, Institute of Zoology, Chinese Academy of Sciences, Beijing 100101, China

[3]School of Life Sciences, Hebei University, Baoding 071002, China

[4]University of Chinese Academy of Sciences, Beijing, 100049, China

[5]Department of Immunology and Infectious Diseases, Harvard T. H. Chan School of Public Health, Boston, Massachusetts 02115, USA

[6]Xinjiang Production and Construction Corps Key Laboratory of Special Fruits and Vegetables Cultivation Physiology and Germplasm Resources Utilization, Agriculture College of Shihezi University, Shihezi 832003, China

[7]Department of Entomology, Texas A&M University, College Station, TX 77843

*Author for correspondence: Feng Ge (Tel: 86-531-66658008, Fax +86-0531-66657914, email: gef@ioz.ac.cn); Yucheng Sun (Tel: 86-10-64807123, Fax +86-10-64807099, email: sunyc@ioz.ac.cn).

Short running title: Transgenerational modulation of wing morph in aphid

**Abstract**

Transgenerational phenotypic plasticity (TPP) refers to the phenomenon that environmental conditions experienced by one generation can influence the phenotype of subsequent generations to adapt to the environment without modification of their DNA sequences. Aphid wing dimorphism is a textbook example of TPP by which a maternal aphid perceives the environmental cues to decide the wing morph of her offspring. However, the signaling mechanism from mother to daughter remains unclear. In this study, we showed that the population density and physical contact caused high proportion of winged offspring in the pea aphid *Acyrthosiphon pisum*. Its *vesicular glutamate transporter 2* (*ApvGluT2*) and *metabotropic glutamate receptor 3* (*ApmGluR3*) were identified by tissue-specific RNA-seq as differentially expressed genes in the head and embryo respectively between solitary and more densely housed maternal aphids. Elevated expression of brain *ApvGluT2* and embryonic *ApmGluR3* led to increases in the winged proportion. Knockdown of either gene inhibited phosphorylation of ApFoxO in embryos. Furthermore, EMSA showed that dephosphorylated ApFoxO directly bound to the promotor of *hedgehog* (*ApHh*), a morphogen gene for wing development, to repress its transcription in stage 20 embryos, causing a lower winged proportion. Our results demonstrated that brain *vGluT2* and embryonic *mGluR3* coordinately relayed the maternal physical contact signals and control wing development in offspring, showcasing a novel regulatory mechanism underlying physical contact-dependent, transgenerational wing dimorphism in aphids.

**Keywords:** Transgenerational phenotypic plasticity, *Acyrthosiphon pisum*, Wing polymorphism, Glutamate signaling, FoxO

## Significance

Transgenerational phenotypic plasticity is a widespread phenomenon that endows organisms and their progenies with abilities to maximize their fitness under different habitats. Aphids exemplify a successful evolutionary strategy through their transgenerational wing dimorphism. We show that transcripts of a vesicular glutamate transporter *vGluT2* in maternal brain and a metabotropic glutamate receptor *mGluR3* in embryo varied in a density-dependent manner and that increased expression of *vGluT2* and *mGluR3* were necessary triggers for signal transduction, leading to production of a high proportion of winged offspring. The *vGluT2-mGluR3* cascade increased the phosphorylation of embryonic FoxO, which released its suppression on *hedgehog* in stage 20 embryos. These findings have brought novel insight into the complicated parent-offspring communications during the wing morph transitions of aphids.

## Introduction

The transgenerational phenotypic plasticity (TPP) is a fascinating capacity of individual genotypes, when experiencing different environmental conditions, to produce different phenotypes in subsequent generations (1). Since the impact of parental experience is expected to persist across generations, the phenotypic adjustment warranted by parents could be beneficial to offspring (2). This process involves detection of environmental cues by a parent, signal delivery, and signal perception by offspring and subsequent alternative phenotypes (1). Parent-to-offspring signaling can be accomplished via mechanisms that are rapid and non-genetic, such as through neurotransmitters, hormones, epigenetic modifications, and microbiota (3).

Insect wing polyphenism is an intrinsic characteristic; a single species can produce flightless (wingless or short-wing) and flight-capable (winged or long-wing) morphs depending on the environment (4-6). Numerous originally winged insect species have become flightless because secondary flight loss favors their adaptation to environmentally stable habitats (7-9). Aphid wing dimorphism is an iconic example of TPP in that maternal aphids perceive the environmental cues, such as population density, nutrients, natural enemy, or even physical contact, and signal the offspring during the embryonic period, by which alate (winged) or apterous (wingless) daughters are destined before birth (10-11). Of the environmental cues, high population density is widely recognized as a biotic stress reflecting the intraspecific competition within habitat, which could reliably drive the transition from wingless to winged aphids across generations (12-13). Since wingless aphids typically have higher fecundity than the

winged morph, switching to the dispersal winged morph from the reproductive morph alleviates resource competition in offspring (13). In some strains of pea aphids, even two maternal aphids housed in a petri dish can efficiently induce a high proportion (>90%) of winged offspring than singly housed aphids (14-16). Physical contact seems to be a trigger for adults to produce winged offspring (14). Similarly, the aphid alarm pheromone can also induce groups of aphids, rather than single individuals, to produce a higher proportion of winged offspring, suggesting that the singly housed aphids that lack physical contact cannot initiate wing morph change in offspring despite perception of the alarm pheromone (17).

Recent studies have identified a number of genes and gene networks involved in the regulation of insect wing polyphenism. In planthoppers, the zinc finger homeodomain transcription factor (Zfh1) and insulin/insulin-like growth factor signaling (IIS) pathways coordinately modulate the fate of wing development in a Forkhead transcription factor subgroup O (FoxO)-dependent manner (18-19). Dephosphorylated FoxO suppresses wing development by inhibiting the transcription of cellular proliferation genes and wing-patterning genes, or through repressing the transcriptional activity of Rotund, a zinc finger transcription factor of wing developmental genes (15, 20-23). However, these mechanisms are within one generation prior to the critical switching time point at the nymphal stage. In contrast, the wing morph of some aphids is determined transgenerationally. Ecdysteroid, miR-9b, dopamine, and IIS signaling in maternal pea aphids are altered by experiencing high population density, which increases the proportion of winged offspring (15, 24-26). In

offspring, the TOR (the target of rapamycin) and Wnt signaling pathways respectively control the occurrence of autophagic and apoptotic degradation of wing disc in 1st instar nymph of pea aphids, resulting in the formation of wingless morph (16, 27). However, the molecules in the brain and embryo that are specifically stimulated by maternal density and determining offspring wing morph before birth are largely unknown.

Glutamate is a primary excitatory neurotransmitter. It not only functions in the signal transduction cascade mediating the parent-offspring communication in the locust, but is involved in the regulation of its interconvertible phase change, from the solitarious to gregarious phase in response to high population density (28). Maintaining an optimal glutamate concentration at the right time and in the right tissue is important for proper nerve cell signaling, and embryo and tissue development. Dysfunctional glutamatergic synaptic transmission has been linked to transgenerational effects on anxiety, fear, pain sensitization, and embryonic development in animals (29-32). Glutamate signaling involves a sophisticated network of metabolic pathways and transport mechanisms that facilitate glutamate synthesis, release, and clearance, ensuring its proper function as the primary excitatory neurotransmitter in the central nervous system (33). This process begins with glutamate production in the presynaptic neurons via the enzyme glutaminase, followed by glutamate sequestration into synaptic vesicles by vesicular glutamate transporters (vGluTs). Upon synaptic activation, glutamate is exocytosed into the synaptic cleft, where it interacts with ionotropic or metabotropic glutamate receptors (iGluRs and mGluRs) on the postsynaptic neuron, triggering a variety of signaling cascades (34).

The glutamate signaling pathway could modify the phosphorylation level of FoxO. Phosphorylated FoxO no longer binds to promoters and thus loses the suppression of the network of wing development genes (18, 35-36). It therefore is plausible that the maternal glutamate pathway controls the phosphorylation level the embryonic FoxO, and thereby regulating the developmental trajectory of wing disc in offspring. In this study, maternal *vesicular glutamate transporter 2* (*ApvGluT2*) and *metabotropic glutamate receptor 3* (*ApmGluR3*) of pea aphids were identified by the tissue-specific RNA-seq as differentially expressed genes; both were induced by physical contact or by high population density. Given the importance of the glutamate signaling pathway in perceiving the population density and transducing the signal to offspring, the effects of brain *ApvGluT2* and embryonic *ApmGluR3* were determined on (i) increases in the proportion of winged offspring, and (ii) FoxO phosphorylation level and downstream wing developmental genes at stage 20 embryo stage, the crucial time point for determination of the wing morph.

## Results

**Physical contact and high maternal density increased the proportion of winged offspring.** To determine the transgenerational effects of maternal density and physical contact on the wing morph in pea aphid offspring, maternal aphids in groups of 1, 2, and 8 were placed in a petri dish respectively, mimicking the solitary, physical contact, and maternal density effects (Figure 1A). Maternal aphids treated with physical contact and high density for 2- and 4-hr had higher proportions of winged offspring than solitary

147 aphids (Figure 1B). Notably, 2- and 4-hrcontacts between two adults resulted in 54.1%
148 and 96.5% winged offspring, similar to the effects of high-density treatment for the
149 same time periods, 86.5% and 94.6% winged offspring, respectively (Figure 1B). Thus
150 physical contact could be utilized to obtain effective induction of winged offspring and
151 even explain the effect achieved by high population density.

152 Since data collected from the two-adult contacting for 2-hr treatment exhibited a
153 full range in percentage of winged offspring from 0% to 100%, the locomotor activity
154 of maternal aphids was traced to determine the possible correlation with the proportion
155 of winged offspring. Three locomotor parameters, including movement distance,
156 velocity, and contact frequency of maternal aphids were monitored by the EthoVision
157 system (Noldus) (Figure S1 A). All three maternal locomotor parameters exhibited
158 strong positive correlations with the winged offspring proportion ($P$ value < 0.0001)
159 (Figure S1 B-D). Furthermore, since movement distance and velocity of maternal
160 aphids were not significantly different between solitary and two-aphid contact for 4-hr
161 treatments, physical contact between maternal aphids could be the key driving factor
162 for higher proportion of winged offspring (Figure S1 E-F).

163 **Physical contact and high density increased the expression of brain *ApvGluT2* and**
164 **embryonic *ApmGluR3* in maternal aphids.** RNA-seq was used to determine tissue-
165 specific gene profiles of solitary maternal aphids and those subjected to 4-hr physical
166 contact treatment. A total of 563 differential expressed genes (DEGs) were identified in
167 maternal heads, while 339 genes were differentially expressed in embryos with the
168 criteria of the absolute value of $Log_2$ (fold change) > 0.58 and $P$ value < 0.05 (Figure

169 1C). Of which, only 6 DEGs functioning in neurotransmitter signaling were identified,
170 including *ApvGluT2* (LOC100168565), *ApmGluR3* (LOC107882629), *Glutamate-*
171 *gated chloride channel α* (*ApGluCl-α*, LOC100162577), *Octopamine receptor β-1R*
172 (*ApOctβ1R*, LOC100166522), *Glycine receptor subunit α1* (*ApGLRA1*,
173 LOC100169196), and *Serotonin receptor 2A* (*ApHTR2A*, LOC100575043) (Figure 1D).
174 qPCR results further confirmed that only head *ApvGluT2* and embryonic *ApmGluR3*
175 had higher transcripts in maternal aphids experiencing physical contact than in solitary
176 aphids (Figure 1E). Furthermore, differential expression of *ApvGluT2* and *ApmGluR3*
177 were not observed in other tissues or in whole body except for gut *ApvGluT2* (Figure
178 1F-G). To validate the involvement of *ApvGluT2* and *ApmGluR3* in perceiving high
179 population density, 15 adults vs. 1 adult were clipped into a plant seedling for 24-hr,
180 and heads and embryos were then dissected and sampled. RT-qPCR showed that 15-
181 adult treatment increased *ApvGluT2* transcripts by 64.9% in the head and *ApmGluR3*
182 transcripts by 34.2% in the embryo relative to solitary aphids (Figure 1H). These results
183 suggested that maternal brain vGluT2 and embryonic mGluR3 were involved in the
184 physical contact-induced production of winged offspring.

185 **Maternal *Ap*v*GluT2* expressed in antennal lobes of aphid brain favored winged**
186 **offspring in a locomotor activity-independent manner.** Previous research showed
187 that neural vGluT2 could modulate animal locomotor activity (37). It was therefore
188 speculated that physical contact-induced *ApvGluT2* in aphid brain may increase the
189 proportion of winged offspring by enhancing the locomotor activity of maternal aphids
190 or by cascading the glutamate pathway to regulate the wing development across

generations. To experimentally test these hypotheses, pharmacological assays were performed on maternal aphids (Figure 2A), followed by monitoring of the locomotor activities and proportion of winged offspring of aphids subjected to 2-adults contact for 2-hr (Figure 2A). Application of glutamate agonist glutamic acid increased winged offspring from 47.6% to 68.1% (Figure 2B). Conversely, vGluT2 inhibitor Chicago Sky Blue (CSB) reduced the proportion of winged offspring from 53.3% to 31.2% (Figure 2F). However, either had any effects on locomotor activities (Figure 2C-E, 2F-I). Fluorescence *in situ* hybridization (FISH) revealed that *ApvGluT2* was mainly expressed in the neural antennal lobes of the aphid brain, and the fluorescent signal intensified as the maternal population density or contact duration increased (Figure 2J-K). Together, aphids activated brain *ApvGluT2* in response to maternal density and physical contact, yet the resulting higher proportion of winged offspring had little to do with the locomotor activity.

**Embryonic *ApmGluR3* relayed the key transgenerational signal involved with wing dimorphism.** Because the embryonic period is a critical time point for determination of offspring wing morph, we hypothesized that *ApmGluR3* in the embryo was a key regulator downstream of *ApvGluT2* that mediated maternal-offspring communication. Application of mGluR antagonist LY341495 decreased the winged offspring by 33% (Figure 3A), whereas injection of mGluR agonist (2R, 4R)-4-aminopyrrolidine-2,4-dicarboxylate (APDC) increased the proportion of winged offspring by 40.4% (Figure 3B). Topical application of ds*ApmGluR3-RNA* knocked down the expression of *ApmGluR3* by 62.2% in the embryo, and the percentage of

213 winged offspring dropped from 56.3% to 36.5% (Figure 3C-E). To establish a causal
214 link between brain vGluT2 and embryo mGluR3, ds*ApvGluT2-RNA* and APDC were
215 administered simultaneously (Figure 3F-G). Notably, reduction of winged offspring
216 caused by the knockdown of *ApvGluT2* diminished upon application of APDC, the
217 agonist of embryonic mGluR3 (Figure 3 F-G). FISH assays revealed abundant
218 *ApmGluR3* in stage 20 embryos (Figure 3H). More importantly, the expression of
219 *ApmGluR3* in the wing disc area of the embryo was up-regulated by density and contact
220 treatments (Figure 3H-I). Presumably, ApmGluR3 functioned downstream of
221 ApvGluT2 in the signaling pathway and mediated transgenerational wing dimorphism
222 during embryonic development.

223 **ApmGluR3 promoted phosphorylation of ApFoxO in embryos.** Our previous study
224 indicated that the embryonic transcription factor, ApFoxO is a crucial suppressor of
225 wing development in pea aphids (15). In planthoppers, phosphorylation of FoxO in
226 wing bud cells caused its translocation from the nucleus to cytoplasm, thereby losing
227 its transcriptional repressor function in wing development (18, 38). We therefore
228 examined whether ApmGluR3 affected phosphorylation of *Ap*FoxO in embryos (Figure
229 4A). Initially, we confirmed that ApFoxO indeed suppressed winged offspring:
230 knockdown of *ApFoxO* in embryos of maternal aphids by 28.6% ($P$ value < 0.0001;
231 Figure 4B) led to a significant increase in the percentage of winged offspring, from
232 53.9% to 61.8% ($P$ value = 0.0255; Figure 4C). Amino acid sequence alignment of
233 ApFoxO with its homologs in fruit fly (DmFoxO) and human (hFoxO4) identified three
234 conserved putative phosphorylation sites in ApFoxO, T15, S187, and S250 (Figure S2).

235 Akt could further phosphorylate these sites to sequestrate FoxO in the cytoplasm, thus
236 preventing FoxO factors from transactivating their target genes (39). Our results found
237 that the phosphorylation of ApFoxO was successfully detected by antibody against
238 phosphorylated T15, but failed to be detected with antibodies targeting phosphorylated-
239 S187 and S250 (Figure 4D-F, S3). Physical contact for 4-hr significantly increased
240 phosphorylated *Ap*FoxO in embryos (by 59.8%) compared to the solitary counterparts
241 (Figure 4D). Knockdown of *ApmGluR3* or *ApvGluT2* reduced the phosphorylation level
242 of ApFoxO in embryos by 21.3% and 54.3%, respectively (Figure 4E-F). In addition,
243 applying the specific Akt inhibitor MK-2206 remarkably reduced the percentage of
244 winged offspring, from 49.8% to 24.9% (Figure 4G). These results implied that the
245 ApvGluT2-ApmGluR3 cascade increased the phosphorylation of ApFoxO in embryos,
246 promoting the winged offspring.

247 **ApFoxO bound to *ApHh* promotor to suppress its activation.** Our previous study
248 found that the transcripts of four wing development genes, including *Hedgehog* (*Hh*),
249 *Vestigial* (*Vg*), *Decapentaplegic* (*Dpp*) and *Mob as tumor suppressor* (*Mats*), were
250 significantly altered by knockdown of *ApFoxO* in the embryos of pea aphids (15). The
251 stage 20 embryo appears to be a critical point in development for an aphid to determine
252 irreversibly its winged or wingless morph (11, 40). Knockdown of *ApmGluR3* at stage
253 20 embryo decreased expression of *ApHh* and *ApMats* by 37.7% and 41.5% (Figure
254 5A). Interestingly, knockdown of *ApFoxO* caused an increase in *ApHh* transcripts, but
255 a decrease in *ApMats* in stage 20 embryos (15). Accordingly, we ruled out *ApMats* and
256 focused on *ApHh* as the suppressing target of ApFoxO. The application of ds*ApHh*-

*RNA* reduced the expression of *ApHh* by 62.4% in stage 20 embryos, and decreased the proportion of winged offspring from 42.5% to 23.5% (Figure 5B-C). Knockdown of *ApFoxO* in stage 20 embryo increased the proportion of winged offspring by 40.4%. Percentage of winged offspring returned to the control level when both *ApFoxO* and *ApHh* were silenced (Figure 5D-E). These findings demonstrated that ApFoxO repressed wing development via inhibiting *ApHh* expression at the $20^{th}$ embryo stage.

Electrophoretic mobility shift assays (EMSA) were then performed to detect binding of ApFoxO to the promotor of *ApHh* via the FoxO recognition element (*FRE*), TTGTTTAC. Typically, FoxO interacts with the *FRE*-element through its highly conserved DNA-binding domain (DBD) consisting of ~100 amino acid residues to regulate transcription of target genes (41-42). The sequence alignment showed that DBD of *ApFoxO* shared high sequence similarity to its homologs in brown planthopper *Nilaparvata lugens*, fruit fly *Drosophila melanogaster* and human *Homo sapiens* (Figure 5F). Two FREs, FRE1 and FRE2, were identified in the 3-kb segment upstream of the transcription start site of *ApHh* (Figure 5G-H). Recombinant maltose-binding protein (MBP)-$DBD_{ApFoxO}$ was expressed in *Escherichia coli* and purified for EMSA (Figure S4). Biotin-labeled probes of FRE2 result in mobility shift in a concentration-dependent manner, while no binding to biotin-labeled FRE1 was detected (Figure 5G-H). Notably, the intensity of shift bands was greatly reduced by adding the unlabeled FRE2 probe. No binding occurred when the cis-element was mutated (Figure 5H), supporting specific interaction between *FRE2* and ApFoxO.

We further compared the temporal expression patterns of *ApHh* between offspring

collected from solitarious and the 4-hr physical contact treatment across the developmental stages from stage 20 embryos to the 4$^{th}$ instar nymphs. Little treatment difference was observed in *ApHh* transcripts in postnatal development stages, suggesting that the stage 20 embryo was a critical time point for decision-making regarding the developmental trajectory of the wing disc (Figure 5I). Together, these findings indicated that embryonic ApFoxO and ApHh were the executors to determine winged dimorphism in aphids.

## Discussion

The phenomenon where a single genotype is expressed in a spectrum of phenotypes, both within a single generation and across successive ones, is central to comprehension of how populations adapt to their environments. This adaptability is particularly complicated in the context of TPP due to its obscure nature of signal transduction mechanisms facilitating parent-offspring communication. Although some understanding has been attained about within-generation wing plasticity in insects, much less is known regarding the transgenerational regulatory mechanism. Our research has demonstrated that maternal brain *ApvGluT2*, mainly expressed in antennal lobes, and embryonic *ApmGluR3* were specifically up-regulated when aphids experienced physical contact or high population density. This was followed by an elevated phosphorylation of *Ap*FoxO in stage 20 embryos, which caused the loss of its suppression of *ApHh*, as well as a high proportion of winged offspring (Figure 6). Conversely, lower expression of *ApvGluT2* and *ApmGluR3* in solitary aphids sustained

a higher level of unphosphorylated ApFoxO, which effectively suppressed *ApHh* expression and favored the production of wingless offspring. These findings showcased how pea aphids deployed the glutamate signaling pathway in regulating transgenerational wing dimorphism in response to environmental cues, and highlighted the importance of the regulatory network of wing development genes in stage 20 embryos.

High population density is a reliable environmental cue for intense competition or deteriorating habitat conditions for individuals, resulting in a high proportion of winged offspring. The tactile, olfactory, and visual signals are essential cues for aphids to perceive population density and trigger appropriate phenotypic changes (43). For instance, physical contact could induce gregarious locusts from a solitary population by releasing aggregation pheromone 4-vinylanisole (28, 44). In aphids, the increased frequency of physical contact due to increasing population density could also explain wing induction (14). A "pseudo-crowding" hypothesis has been proposed to explain the predator-induced wing induction in aphids. The perception of predators or the alarm pheromone increases the locomotion activity of aphids, causing higher frequency of physical contact among individuals, similar to what happens when aphids are crowded. Although single individuals could behaviorally react to the alarm pheromone, lack of physical contact renders them unable to trigger wing production (17). Consistently, aphids with ablated antennae fail to produce more winged offspring in the presence of predators (17). Our previous screening of natural pea aphids gave rise to a strain that was highly sensitive to physical contact in triggering winged offspring, which provided

an excellent biotype for dissecting the underlying molecular mechanism (16). Our results found a strong correlation between the locomotor activity of maternal aphids and the proportion of winged offspring in the treatment of two-adult contacting for 2-hr. Presumably, elevated mobility of maternal aphids led to higher frequency of physical contact, in agreement with the pseudo-crowding hypothesis.

Low titers of serotonin, dopamine and octopamine are found in densely populated pea aphids (45). Of these biogenic amines, only dopamine was reported to be a suppressor for winged morph production (24). In this study, physical contact stimulated higher transcription activity of *ApvGluT2* mainly located in the antennal lobes of the maternal brain. Blocking the vGluT2 activity reduced the proportion of winged offspring but did not alter maternal locomotor activity. It has been shown that vGluTs are essential in sensing mechanical pain in somatosensory system, dorsal horn and brain (46). As evidenced by transiently expressing *vGluT3* in neurons of mammal deep dorsal horn, it could directly receive Aβ primary sensory input caused by mechanical stimuli, and relay polysynaptic transmission onto lamina I pain processing neurons (47-48). Our phylogenetic analysis and sequence alignment indicated that ApvGluT2 belonged to animal Clade III in the solute carrier (SLC) 17 subfamily, sharing 21.33%, 22.33%, and 20.74% amino acid identity with human vGluT1, vGluT2, and vGluT3, respectively, along with 12 conserved transmembrane regions (Figure S5 A-B). Notably, ApvGluT2 exhibited a significant structural similarity to human vGluT2, as evidenced by minimal root mean square deviation (RMSD) value of 4.131 Å, suggesting ApvGluT2 maintained relatively conserved function in aphids (Figure S5 C). Most likely, a specific

group of *ApvGluT2*-expressing neurons in antennal lobes of aphids received physical contact-induced sensory input, then transmitted the synaptic signals to downstream nerves to modulate the offspring wing morph at their embryonic period.

Considering that the antennal lobes are located at a considerable distance from the embryos, an important issue is how the brain ApvGluT2 controls the wing development trajectory in embryos. Our results revealed that the embryonic *ApmGluR3* was up-regulated by maternal high density and physical contact experiences. Although *ApmGluR3* was expressed throughout the embryo, it could be up-regulated by density and contact treatments in the area of wing discs. Injection of mGluR agonist rescued the negative effect of ds*ApvGluT2* on the proportion of winged offspring, suggesting *ApvGluT2* and *ApmGluR3* coordinately regulated the production of wing morph in offspring triggered by maternal density. Early studies have shown that the vGluT-mGluR signal axis orchestrates the function of specific neuronal networks involved in motor coordination, emotions, and cognition (49). Furthermore, the glutamatergic neurons in the ventral nerve cord and thoracic abdominal ganglion could project to the reproductive tract to regulate reproduction (50-52). Therefore, it is likely that glutamatergic neurons in antennal lobes of aphids recruited vGluT2-mediated signaling to activate the glutamatergic neurons in the ventral nerve cord and thoracic abdominal ganglion, innervating the mGluR3-expressed cells in the wing disc of embryos to control their wing development.

Although FoxO acts as a major suppressor of the winged morph in both within- and trans-generational wing polyphenism, the regulatory routes may vary in

367 developmental stages by targeting different downstream wing development genes.
368 Some such as *Vg* and *Ubx* that control the wing patterning in wing buds could be
369 suppressed by FoxO within a generation (23, 53). As for the transgenerational
370 regulation, we showed that physical contact-induced increases of brain *ApvGluT2* and
371 embryonic *ApmGluR3* enhanced the phosphorylation level of ApFoxO, as well as the
372 proportion of winged offspring. In contrast, knockdown of *ApvGluT2* and *ApmGluR3*,
373 and the application of Akt antagonist could reduce the phosphorylation level of ApFoxO,
374 consistent with a previous study, where mGluR activates PI3K in *Drosophila* larval
375 motor neuron to alter phosphorylation of FoxO (35). Furthermore, we demonstrated
376 that FoxO could directly bind to the promotor of *ApHh* to suppress its expression in
377 stage 20 embryos, a critical development stage for wing morph. *Hh* gene encodes a
378 morphogen to form a concentration gradient which confers the positional information
379 to wing disc cells, and determines wing developmental trajectory (54-55). Together, we
380 have provided a novel mechanistic insight into the regulation of TPP and demonstrated,
381 for the first time that the glutamate signal transduction cascade mediates the
382 transgenerational wing dimorphism in aphids.
383

384 **Materials and methods**

385 **Aphid rearing.** The pea aphid *A. pisum* (strain: Ningxia Red) was originally collected
386 from *Medicago sativa* in Ningxia Province and had been reared in the laboratory for
387 over 8 years. Nymphs from the same parthenogenetic pea aphid female were reared on
388 *Vicia faba* at 18-20°C, with 60% relative humidity and a photoperiod of a 16 hr: 8 hr

(light/dark) cycle. To eliminate the transgenerational effects on offspring morphs, females were maintained at low density (three per plant) on *V. faba* seedlings for more than three generations (14). This strain was used to test the effects of two-adult physical contact or crowding on the proportion of winged offspring.

**Induction of winged offspring.** To effectively induce a high proportion of winged offspring, the maternal density and contacting duration were evaluated in petri dishes (35 mm in diameter) as described by 14. Three groups of aphids consisting of 1, 2, or 8 wingless adults, respectively, were placed in a petri dish for 0.5-, 2-, and 4-hr. After treatment, each adult was transferred to a freshly detached *V. faba* leaf kept in petri dishes with 1% agar to reproduce for 24-hr. After newborns reached the fourth instar, the proportion of winged offspring from each adult was calculated.

For density treatment, two groups of 1 and 15 maternal aphids were placed on fava seedlings for 24-hr. This was followed by transferring each adult to a fresh *V. faba* leaf as described above.

**Aphid locomotor activity tracking in petri dishes.** One or two maternal aphids were placed in a petri dish (diameter 35 mm), and locomotor activities of each aphid within 2- or 4-hr were recorded (25 frames/s) with a video camera. Six or 12 aphids in each treatment were simultaneously recorded per replicate. The valid video data for each treatment were collected and analyzed at least 40 replicates. Videos were analyzed using the EthoVision XT software (v.11.5, Noldus Information Technology) to measure the total distance (moving distance, unit: cm) and the average velocity of movement (move velocity, unit: cm/s), as well as the contact frequency. Physical contact between

411 two maternal aphids was considered to have occurred when their proximity distance
412 was less than 0.5 cm.

413 **RNA-Seq.** Maternal aphids housed individually or two per petri dish for 4-hr were used
414 for differential gene expression analyses. The heads and embryos were dissected from
415 10 and 5 adult aphids per replicate, respectively. Four of such biological replicates were
416 collected RNA-seq. DEGs were identified with DESeq2 R package (1.20.0) using the
417 expected number of Fragments Per Kilobase of transcript sequence per Million base
418 pairs sequenced. The sequencing data were deposited in the Short Read Archive (NCBI)
419 under accession number PRJNA1017088.

420 **RT-qPCR.** Total RNA was extracted using TRIzol reagent (Invitrogen, CA, USA), and
421 reverse transcribed using the PrimeScriptTM RT reagent Kit with gDNA Eraser (Perfect
422 Real Time) kit (Takara, Dalian, China). The RT-qPCR reactions were carried out on the
423 PikoReal 96 Real-Time PCR System (Thermo) using the SuperReal PreMix Color
424 (SYBR Green) kit (Tiangen, Beijing, China). Three technical replicates were applied
425 for each biological replicate. The housekeeping gene ribosomal protein L27 (RPL27)
426 was used as the internal qPCR standard.Gene expression data were analyzed by relative
427 quantification with the $2^{-\triangle\triangle CT}$ method (56). Specific primers for each gene were
428 designed using Primer Premier 6 and tested in preliminary experiments. The
429 oligonucleotides are listed in Table S1.

430 **Pharmacological experiments.** Glutamate signaling agonist glutamic acid
431 (Topscience, Shanghai) and mGluR agonist (2R, 4R)-ADPC (Enzo Life Sciences, New
432 York) were dissolved in water at concentrations of 33.98 mM and 100 nM, respectively.

433 vGluT2 antagonist Chicago Sky Blue 6B (CSB) (Topscience, Shanghai), mGluR
434 antagonist LY341495 (MedChemExpress, New Jersey), and Akt inhibitor MK-2206
435 (Selleckchem, Houston) were dissolved in DMSO at concentrations of 10 mM, 16.98
436 mM, and 5 mM, respectively. A volume of 100 nL of each chemical, except for MK2206,
437 which was 23.6 nL, was delivered into hemolymph from dorsal abdomens using the
438 Nanoject II microinjection system (Drummond Scientific Company, Broomall, PA,
439 USA). An equivalent amount of solvent was used as a solvent control.

440 **Fluorescence in situ hybridization.** FISH was performed with the technique modified
441 by Kliot et al. (2014). After washing in TBST (TBS with 0.2% Triton-X) for 10 min,
442 sample section slices were rinsed three times in the hybridization buffer (20 mM Tris-
443 HCl, pH 8.0, 0.9 M NaCl, 0.01% sodium dodecyl sulfate, and 30% formamide), and
444 hybridized overnight in the hybridization buffer containing 10 pmol of the fluorescent
445 RNA probe (conjugated with FAM or Cy5). After 3x rinses in TBST, samples were
446 mounted in Fluoroshield Mounting Medium with DAPI (Abcam). Sections were
447 imaged using a Leica M205C confocal microscope (Zeiss, Germany).

448 **RNA interference.** Double-stranded RNA (dsRNAs) i.e. ds*ApvGluT2*, ds*ApmGluR3*,
449 ds*ApFoxO*, ds*ApHh*, and the ds*GFP* control were synthesized by T7 RiboMAX Express
450 RNAi System (Promega, P1700) according to the manufacturer's protocol. Each (2
451 μg/μl) was mixed with the nanocarrier in a water solution at a volume ratio of 1:1. A
452 volume of 1 μL of the solution containing 1 μg nanocarrier/dsRNA complex was
453 topically applied to the dorsal side of the female abdomen. Embryos from aphids or
454 heads from ten aphids in each sample were collected 24 h after topical application of

455 dsRNA for testing silencing efficiency using qPCR. Each treatment contained at least
456 three biological replicates.

457 **Antibody preparation and western blotting analysis.** Three polyclonal rabbit
458 antibodies against phosphorylated T15, S187 and S250 of ApFoxO were prepared by
459 ABclonal using synthetic peptides RARSNT(p)WPLPR (10 to 20 aa),
460 RRRAVS(p)METPK (182 to 192 aa) and RARASS(p)NASS (245 to 254 aa) as the
461 immunogens. Western blotting was performed to detect phosphorylation levels of FoxO
462 in embryos of adult females. The antigen–antibody complexes were visualized using a
463 secondary goat anti-rabbit IgG (H+L)-conjugated horseradish peroxidase (HRP)
464 antibody (LABLEAD).

465 **Electrophoretic mobility shift assays (EMSA).** The FoxO DNA-binding domain
466 (DBD) (89 to 178 aa) was cloned into the pMAL-c2x expression vector, which
467 contained an N-terminal maltose-binding protein (MBP), and subsequently expressed
468 in *E. coli* strain Rosetta (DE3). Proteins were purified from cell lysates using the pMAL
469 protein fusion and purification system (New England Biolabs). The MBP protein was
470 also independently expressed in pMAL-c2x as control. EMSA was conducted as
471 described previously (57). Probes containing the DBD binding sites were labeled with
472 biotin at the 5' end. Unlabeled probe was used as the competitor. The probes were
473 incubated with purified MBP/DBD recombinant protein at room temperature for 30
474 min, run on a non-denaturing 0.5×TBE 6% polyacrylamide gel for 1h (60 V at 4°C),
475 and transferred onto Biodyne® B nylon membrane (Pall Corporation). Signals were
476 visualized using the ChemiDoc XRS kit (Bio-Rad Laboratories, UAS).

**Phylogenetic construction of SLC17 proteins.** Protein sequences, 333 from 10 different species, were obtained from UniProt (https://www.uniprot.org/). Sequences were aligned with MAFFT v7.310 (58) and automated trimmed with trimAl v1.4 (59). Phylogenetic analysis was performed using IQ-TREE v2.0.3 with LG+R9 model and ultrafast bootstrap approximation with 1000 replicates (60). Phylogenetic tree was visualized in Interactive Tree Of Life (iTOL) (61).

**Protein Sequence and Structure analysis.** The multiple sequence alignment was performed using Multiple Protein Sequence Alignment (MUSCLE). High confidence protein structure of *Ap*vGluT2 was predicted by Alphafold v2.3.0 (62). The pairwise structural alignments were performed using PyMOL 2.6.0a0 (*www.pymol.org*).

**Statistical Analyses.** The GraphPad software was used for statistical analyses. All data were checked for normality by the Wilk–Shapiro test. Two-tailed unpaired t-test was used to separate the means of normally distributed data, while Mann–Whitney test was used to analyze nonparametric data. All western blotting and confocal assays were repeated independently at least three times with similar results. Pearson's correlations were calculated to determine the relationship between proportion of winged offspring and maternal locomotor activities.

## Data Availability

All data used in the study are included, and some are presented as supplementary information. All protocols have been described in Materials and Methods or in the references therein. No custom codes or mathematical algorithms were used in this manuscript.

## Author contribution

Yiyang Yuan project designing, performing experiments, data analysis and manuscript writing; Yanyan Wang, Wanwan Ye, Liqiang Xie, Fang Dong performing experiments; Keyan Zhu-Salzman manuscript writing and revising, and Erliang Yuan, Huijuan Guo, Shifan Wang manuscript revising; Feng Ge, Yucheng Sun project designing and coordination, manuscript writing.

## Declare of interests

We declare no competing interest.

## Acknowledgements

We thank Prof. Jinfeng Chen for his support in phylogenetic analysis. This project was supported by the National Key R&D Program of China (no. 2023YFD1400800), the Taishan Scholars Program, the Agricultural Science and Technology Innovation Project of the Shandong Academy of Agricultural Sciences (no. CXGC2023F04), the National Natural Science Foundation of China (nos. 31970453, 32250002 and 32372636), and the State Key Laboratory of Integrated Management of Pest Insects and Rodents (no. IPM2306).

## References

1. A.-M Bell, J.-K Hellmann, An integrative framework for understanding the mechanisms and multigenerational consequences of transgenerational plasticity. Annu. Rev. Ecol. Evol. Syst. 50, 97–118 (2019).

2. A.-S. Guillaume, K. Monro, D.-J. Marshall, Transgenerational plasticity and environmental stress: do paternal effects act as a conduit or a buffer? Funct. Ecol. 30, 1175–1184 (2016).

3. S.-C. Donelan, et al., Transgenerational Plasticity in Human-Altered Environments. Trends Ecol. Evol. 35, 115–124 (2020).

4. J.-A. Brisson, Aphid wing dimorphisms: linking environmental and genetic control of trait variation. Philos. Trans. R. Soc. B, Biol. Sci. 365, 605–616 (2010).

5. A.-J. Zera, R.-F. Denno, Physiology and ecology of dispersal polymorphism in insects. Annu. Rev. Entomol. 42, 207–230 (1997).

6. C.-X. Zhang, J. A. Brisson, H.-J. Xu, Molecular Mechanisms of Wing Polymorphism in Insects. Annu. Rev. Entomol. 64, 297–314 (2019).

7. D.-A. Roff, The evolution of flightlessness in insects. Ecol. Monogr. 60, 389–421 (1990).

8. D.-L. Wagner, J.-K. Liebherr, Flightlessness in insects. Trends Ecol. Evol. 7, 216–220 (1992).

9. D.-A. Roff, The evolution of flightlessness: Is history important? Evol. Ecol. 8, 639–657 (1994).

10. C. Braendle, I. Friebe, M.-C.Caillaud, D.-L.Stern,. Genetic variation for an aphid

wing polyphenism is genetically linked to a naturally occurring wing polymorphism. Proc. Biol. Sci. 272, 657–664 (2005).

11. A. Ishikawa, T. Miura, Transduction of high-density signals across generations in aphid wing polyphenism. Physiol. Entomol. 38, 150–156 (2013).

12. O. Sng, J. M. Ackerman, Too many people, women, men? The psychological effects of population density and sex ratio. Curr Opin Psychol 32, 38–42 (2020).

13. K.-D. Deem, L.-E. Gregory, X. Liu, O.-S. Ziabari, J.-A. Brisson, Evolution and molecular mechanisms of wing plasticity in aphids. Curr Opin Insect Sci 61, 101142 (2024).

14. O. R. W. Sutherland, The role of crowding in the production of winged forms by two strains of the pea aphid, Acyrthosiphon pisum. J. Insect Physiol. 15, 1385–1410 (1969).

15. Y. Yuan, et al., Functional evaluation of the insulin/insulin-like growth factor signaling pathway in determination of wing polyphenism in pea aphid. Insect Sci. 30, 816–828 (2023).

16. E. Yuan, et al., A novel gene REPTOR2 activates the autophagic degradation of wing disc in pea aphid. Elife 12 (2023).

17. G. Kunert, S. Otto, U.-S.-R. Röse, J. Gershenzon, W.-W. Weisser, Alarm pheromone mediates production of winged dispersal morphs in aphids. Ecol. Lett. 8, 596–603 (2005).

18. H.-J. Xu, et al., Two insulin receptors determine alternative wing morphs in planthoppers. Nature 519, 464–467 (2015).

19. J.-L. Zhang, S.-J. Chen, X.-Y. Liu, A. P. Moczek, H.-J. Xu, The transcription factor Zfh1 acts as a wing-morph switch in planthoppers. Nat. Commun. 13, 5670 (2022).

20. S.-J. Chen, et al., FoxO and rotund form a binding complex governing wing polyphenism in planthoppers. iScience 26, 107182 (2023).

21. X. Lin, et al., Cell cycle progression determines wing morph in the polyphenic insect Nilaparvata lugens. iScience 23, 101040 (2020).

22. N. Xu, S.-F. Wei, H.-J. Xu, Transcriptome Analysis of the Regulatory Mechanism of FoxO on Wing Dimorphism in the Brown Planthopper, Nilaparvata lugens (Hemiptera: Delphacidae). Insects 12 (2021).

23. J.-L. Zhang, et al., Vestigial mediates the effect of insulin signaling pathway on wing-morph switching in planthoppers. PLoS Genet. 17, e1009312 (2021).

24. X. Liu, J.-A. Brisson, Dopamine mediates the pea aphid wing plasticity. Biol. Lett. 19, 20230024 (2023).

25. F. Shang, et al., The miR-9b microRNA mediates dimorphism and development of wing in aphids. Proc. Natl. Acad. Sci. U. S. A. 117, 8404–8409 (2020).

26. N.-N. Vellichirammal, P. Gupta, T.-A. Hall, J.-A. Brisson, Ecdysone signaling underlies the pea aphid transgenerational wing polyphenism. Proc. Natl. Acad. Sci. U. S. A. 114, 1419–1423 (2017).

27. P. Zhou, et al., The Wnt pathway regulates wing morph determination in Acyrthosiphon pisum. Insect Biochem. Mol. Biol. 161, 104003 (2023).

28. J. Yang, Q. Yu, J. Yu, L. Kang, X. Guo, 4-Vinylanisole promotes conspecific interaction and acquisition of gregarious behavior in the migratory locust. Proc. Natl.

Acad. Sci. U. S. A. 120, e2306659120 (2023).

29. Y. Liu, et al., Activity strengths of cortical glutamatergic and GABAergic neurons are correlated with transgenerational inheritance of learning ability. Oncotarget 8, 112401–112416 (2017).

30. W. Tao, et al., MeCP2 mediates transgenerational transmission of chronic pain. Prog. Neurobiol. 189, 101790 (2020).

31. S.-K. Jones, et al., Transgenerational transmission of aspartame-induced anxiety and changes in glutamate-GABA signaling and gene expression in the amygdala. Proc. Natl. Acad. Sci. U. S. A. 119, e2213120119 (2022).

32. L.-J. Van Winkle, Perspective: Might Maternal Dietary Monosodium Glutamate (MSG) Consumption Impact Pre- and Peri-Implantation Embryos and Their Subsequent Development? Int. J. Environ. Res. Public Health 19 (2022).

33. D.-E. Featherstone, Intercellular glutamate signaling in the nervous system and beyond. ACS Chem. Neurosci. 1, 4–12 (2010).

34. S.-S. Willard, S. Koochekpour, Glutamate, glutamate receptors, and downstream signaling pathways. Int. J. Biol. Sci. 9, 948–959 (2013).

35. E. Howlett, C.-C.-J. Lin, W. Lavery, M. Stern, A PI3-kinase-mediated negative feedback regulates neuronal excitability. PLoS Genet. 4, e1000277 (2008).

36. B. Zhang, et al., Brain-gut communications via distinct neuroendocrine signals bidirectionally regulate longevity in *C. elegans*. Genes Dev. 32, 258–270 (2018).

37. D. M. Roccaro-Waldmeyer, et al., Eliminating the VGlut2-Dependent Glutamatergic Transmission of Parvalbumin-Expressing Neurons Leads to Deficits in

Locomotion and Vocalization, Decreased Pain Sensitivity, and Increased Dominance. Front. Behav. Neurosci. 12, 146 (2018).

38. X. Lin, Y. Yao, B. Wang, D.-J. Emlen, L.-C. Lavine, Ecological Trade-offs between Migration and Reproduction Are Mediated by the Nutrition-Sensitive Insulin-Signaling Pathway. Int. J. Biol. Sci. 12, 607–616 (2016).

39. D.-R. Calnan, A. Brunet, The FoxO code. Oncogene 27, 2276–2288 (2008).

40. K. Ogawa, T. Miura, Two developmental switch points for the wing polymorphisms in the pea aphid *Acyrthosiphon pisum*. Evodevo 4, 30 (2013).

41. T. Furuyama, T. Nakazawa, I. Nakano, N. Mori, Identification of the differential distribution patterns of mRNAs and consensus binding sequences for mouse DAF-16 homologues. Biochem. J 349, 629–634 (2000).

42. Z. Xuan, M.-Q. Zhang, From worm to human: bioinformatics approaches to identify FOXO target genes. Mech. Ageing Dev. 126, 209–215 (2005).

43. C. M. Topaz, M. R. D'Orsogna, L. Edelstein-Keshet, A. J. Bernoff, Locust dynamics: behavioral phase change and swarming. PLoS Comput. Biol. 8, e1002642 (2012).

44. X. Guo, et al., 4-Vinylanisole is an aggregation pheromone in locusts. Nature 584, 584–588 (2020).

45. N.-N. Vellichirammal, N. Madayiputhiya, J.-A. Brisson, The genomewide transcriptional response underlying the pea aphid wing polyphenism. Mol. Ecol. 25, 4146–4160 (2016).

46. R.-P. Seal, Do the distinct synaptic properties of VGLUTs shape pain? Neurochem. Int. 98, 82–88 (2016).

47. C. Peirs, et al., Dorsal Horn Circuits for Persistent Mechanical Pain. Neuron 87, 797–812 (2015).

48. R.-P. Seal, et al., Injury-induced mechanical hypersensitivity requires C-low threshold mechanoreceptors. Nature 462, 651–655 (2009).

49. K.-S. Ibrahim, K.-S. Abd-Elrahman, S.-El Mestikawy, S.-S.-G. Ferguson, Targeting Vesicular Glutamate Transporter Machinery: Implications on Metabotropic Glutamate Receptor 5 Signaling and Behavior. Mol. Pharmacol. 98, 314–327 (2020).

50. R. Rodríguez-Valentín, et al., Oviduct contraction in Drosophila is modulated by a neural network that is both, octopaminergic and glutamatergic. J. Cell. Physiol. 209, 183–198 (2006).

51. M.-C. Castellanos, J.-C.-Y. Tang, D.-W. Allan, Female-biased dimorphism underlies a female-specific role for post-embryonic Ilp7 neurons in Drosophila fertility. Development 140, 3915–3926 (2013).

52. S.-A. Deshpande, et al., Regulation of Drosophila oviduct muscle contractility by octopamine. iScience 25, 104697 (2022).

53. F. Liu, et al., Ultrabithorax is a key regulator for the dimorphism of wings, a main cause for the outbreak of planthoppers in rice. Natl Sci Rev 7, 1181–1189 (2020).

54. T.-A. Hartl, M.-P. Scott, Wing tips: The wing disc as a platform for studying Hedgehog signaling. Methods 68, 199–206 (2014).

55. R.-M. Neto-Silva, B.-S. Wells, L.-A. Johnston, Mechanisms of growth and homeostasis in the Drosophila wing. Annu. Rev. Cell Dev. Biol. 25, 197–220 (2009).

56. K. J. Livak, T. D. Schmittgen, Analysis of relative gene expression data using real-

time quantitative PCR and the $2^{-\triangle\triangle CT}$ Method. Methods 25, 402–408 (2001).

57. L. M. Hellman, M. G. Fried, Electrophoretic mobility shift assay (EMSA) for detecting protein-nucleic acid interactions. Nat. Protoc. 2, 1849–1861 (2007).

58. K. Katoh, K. Misawa, K.-I. Kuma, T. Miyata, MAFFT: a novel method for rapid multiple sequence alignment based on fast Fourier transform. Nucleic Acids Res. 30, 3059–3066 (2002).

59. S. Capella-Gutiérrez, J.-M. Silla-Martínez, T. Gabaldón, trimAl: a tool for automated alignment trimming in large-scale phylogenetic analyses. Bioinformatics 25, 1972–1973 (2009).

60. B. Q. Minh, et al., IQ-TREE 2: New Models and Efficient Methods for Phylogenetic Inference in the Genomic Era. Mol. Biol. Evol. 37, 1530–1534 (2020).

61. I. Letunic, P. Bork, Interactive Tree Of Life (iTOL) v5: an online tool for phylogenetic tree display and annotation. Nucleic Acids Res. 49, W293–W296 (2021).

62. J. Jumper, et al., Highly accurate protein structure prediction with AlphaFold. Nature 596, 583–589 (2021).

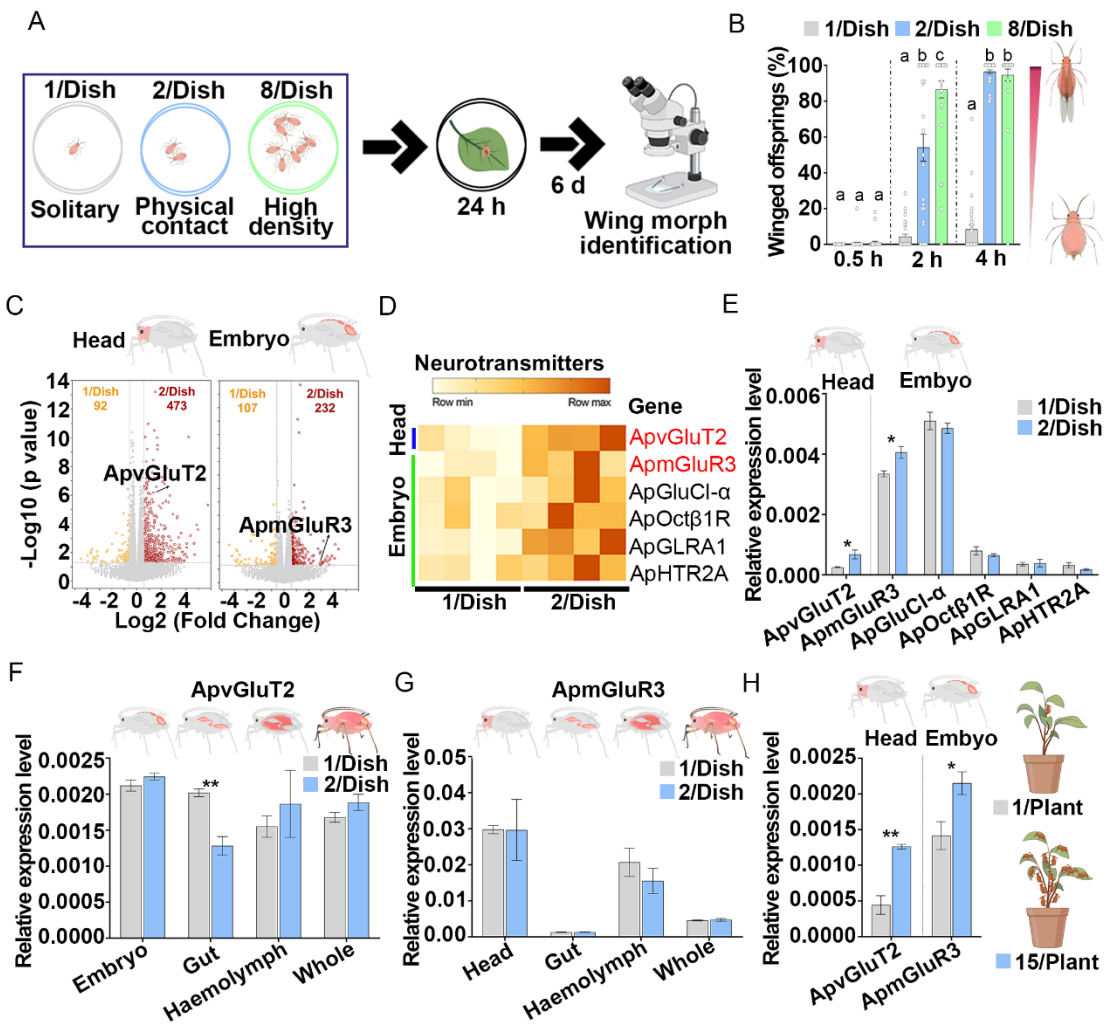


**Figure 1 Maternal aphids produced high proportions of winged offspring after experiencing physical contact and high density, with increased expression of head *ApvGluT2* and embryo *ApmGluR3*.** (A) The schematic procedure of transgenerational induction of winged offspring. (B) Effects of maternal density and duration on the proportion of winged offspring (n=32). Two-adult contact for 4 hr was sufficient to induce over 90% of winged offspring. Kruskal-Wallis test was performed, and Dunn's test was used to differentiate between the means; different letters indicate significant differences ($P < 0.05$). (C) The volcano plots showing differentially expressed genes (DEGs) in the head and embryo induced by two-adult contacting for 4-hr (n=4). DEGs were selected if the absolute value of $Log_2$ (Fold change) > 0.58 and $P < 0.05$. (D) The

heat map showing the expression patterns of six DEGs functioning in neurotransmitter signaling in RNAseq analyses (n=4). (E) qPCR confirmation of increased expression of *ApvGluT2* and *ApmGluR3* in head and embryo, respectively caused by maternal physical contact (n=3). (F) The tissue-specific expression of *ApvGluT2* and (G) *ApmGluR3* in two-adult contacting for 4-hr treatment vs. solitary treatment (n=3). (H) Transcripts of head *ApvGluT2* and embryo *ApmGluR3* were higher in group aphids of 15 adults than those of singly kept aphids on plants, as determined by qPCR (n=3). Student *t* test: *P < 0.05, **P < 0.01.

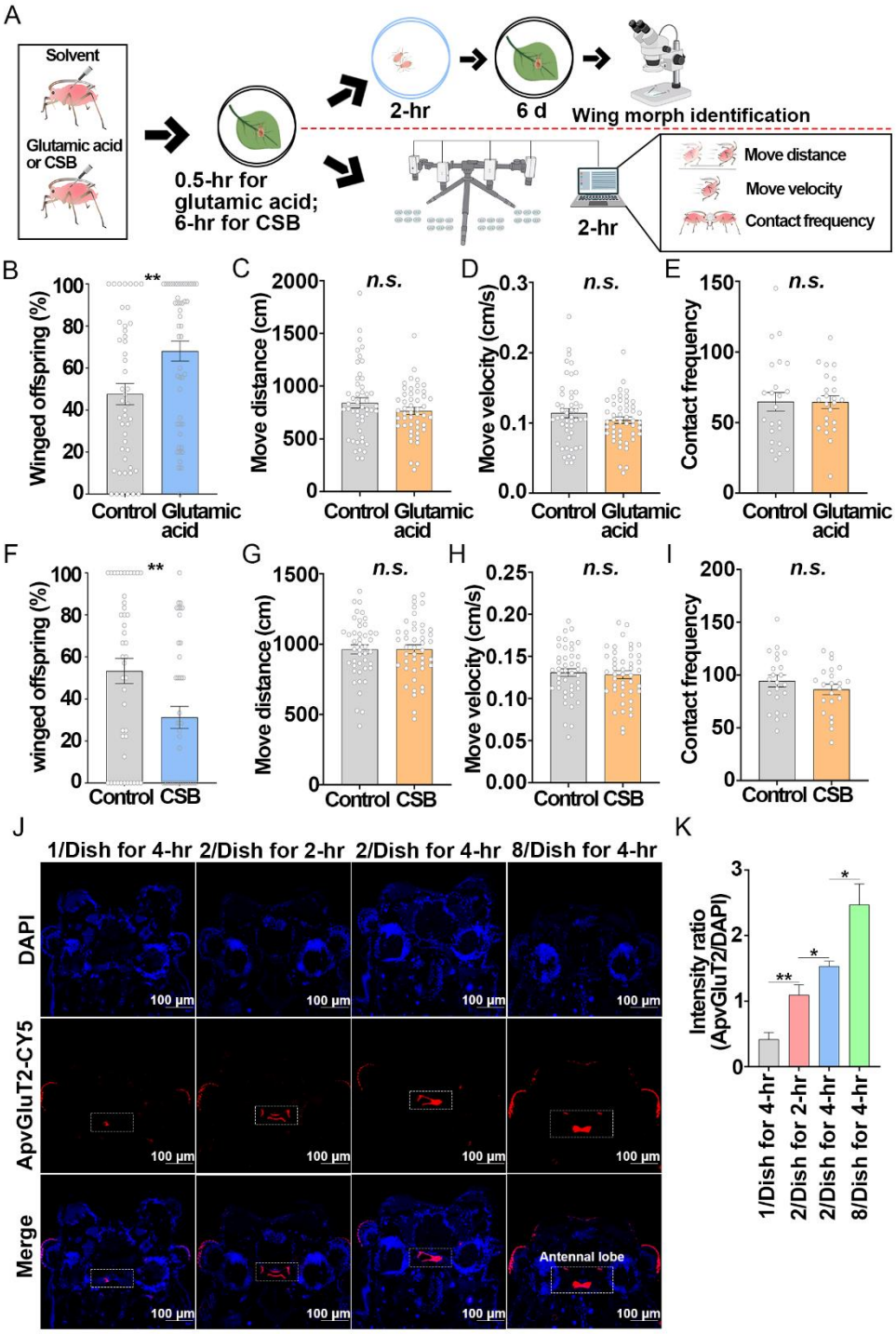


683

684 **Figure 2 The effect of *ApvGluT2* on the proportion of winged offspring and its**

685 **location in aphid brain.** (A) Schematic diagram showing the procedure of winged

686 offspring inspection and behavior monitoring in pharmacological experiments in pea

687 aphids. (B) Increased percentage of winged offspring by glutamic acid injection, an

agonist of vGluT (n>47). (C) The effect of glutamic acid injection on the movement distance (n=48), (D) the movement velocity (n = 48), and (E) the contact frequency of maternal aphids (n=24). The Kolmogorov-Smirnov test was used to compare means. (F) Decreased percentage of winged offspring by CSB injection, an antagonist of vGluT (n>42). (G) The effect of CSB injection on the movement distance (n=44), (H) the movement velocity (n=44), and (I) the contact frequency of maternal aphids (n=22). (J) mRNA-FISH. *ApvGluT2* was mainly expressed in the neural antennal lobes (highlighted by white squares) of aphid brain and was induced by high maternal density and contact treatments. Cy5-conjugated *ApvGluT2* probe was shown in red, and nuclei were stained with DAPI in blue. (K) The relative intensity of *ApvGluT2* in the antennal lobes was quantified by LAS X (n >6). The Mann Whitney non-parametric test was used to compare means of the proportions of winged offspring. Student *t* test was used to compare means of relative intensity of *ApvGluT2*. *n.s.*, not significant, *P < 0.05, **P < 0.01.

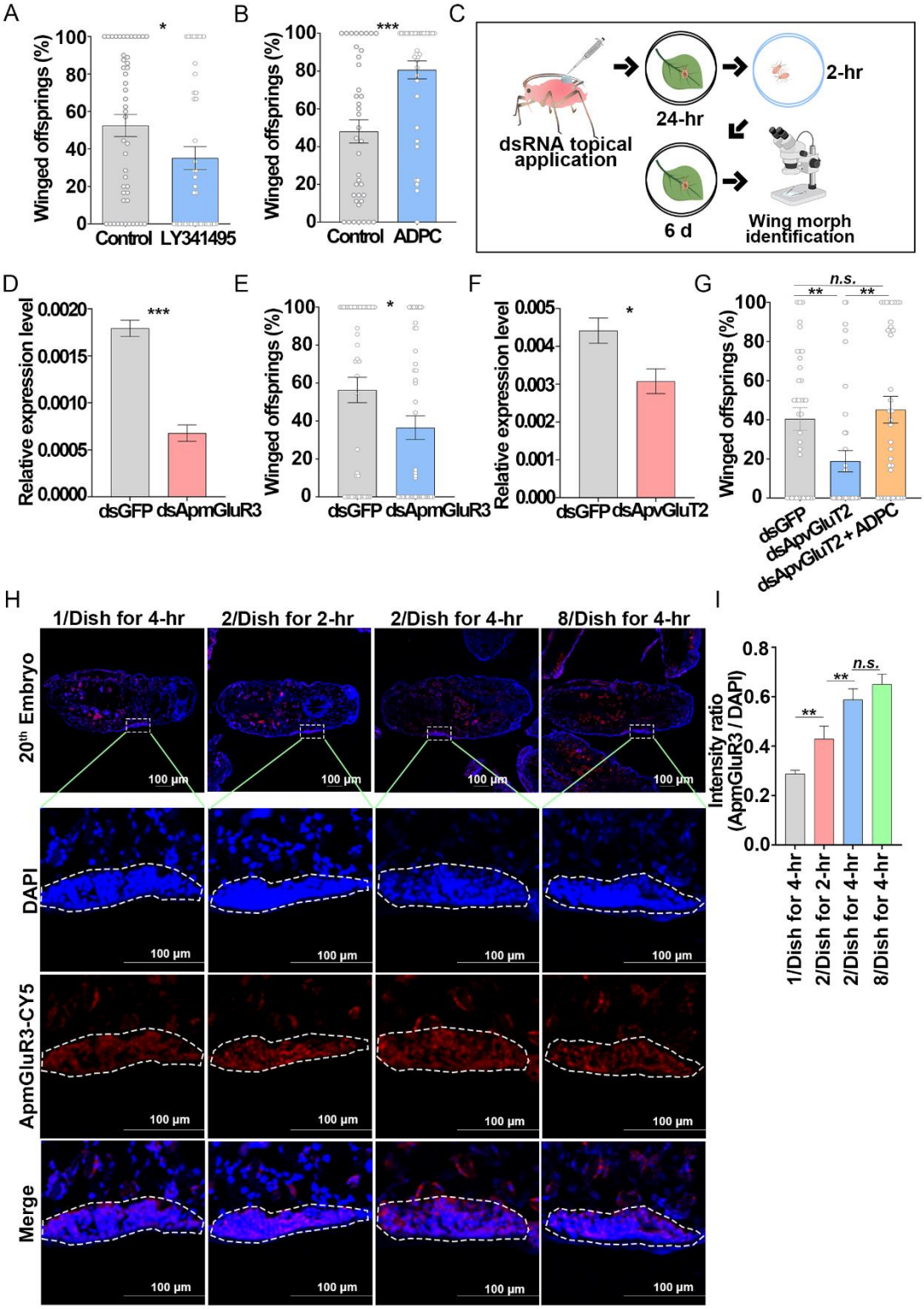


**Figure 3 Embryonic *ApmGluR3* relayed the transgenerational signal from *ApvGluT2* about the induction of winged offspring.** (A) Declined proportion of winged offspring by injection of an mGluR antagonist LY341495 (n=47), in contrast to

706 (B) increased proportion by agonist ADPC (n=39). (C) RNAi experimental design. (D)
707 Knockdown of *ApmGluR3* in the embryo (n=3), and (E) reduced proportion of winged
708 offspring (n=47). (F) RNAi efficiency of *ApvGluT2* in the head (n=4). (G) Effect of
709 ds*ApvGluT2* on the proportion of winged offspring was rescued by ADPC (n=36). (H)
710 The expression of *ApmGluR3* in the stage 20 embryos increased as the contact duration
711 increased. *ApmGluR3* probe conjugated with Cy5 was in red, and nuclei were stained
712 with DAPI in blue. Wing discs shown in confocal were highlighted by white circles. (I)
713 The relative intensity of *ApmGluR3* in the wing discs of stage 20 embryos was
714 quantified by LAS X (n>9). Mann Whitney non-parametric test was used to compare
715 the means of the proportion of winged offspring. Student *t* test was used to compare
716 means of transcript level or the relative intensity of *ApmGluR3*. *P < 0.05, **P < 0.01,
717 ***P < 0.001.

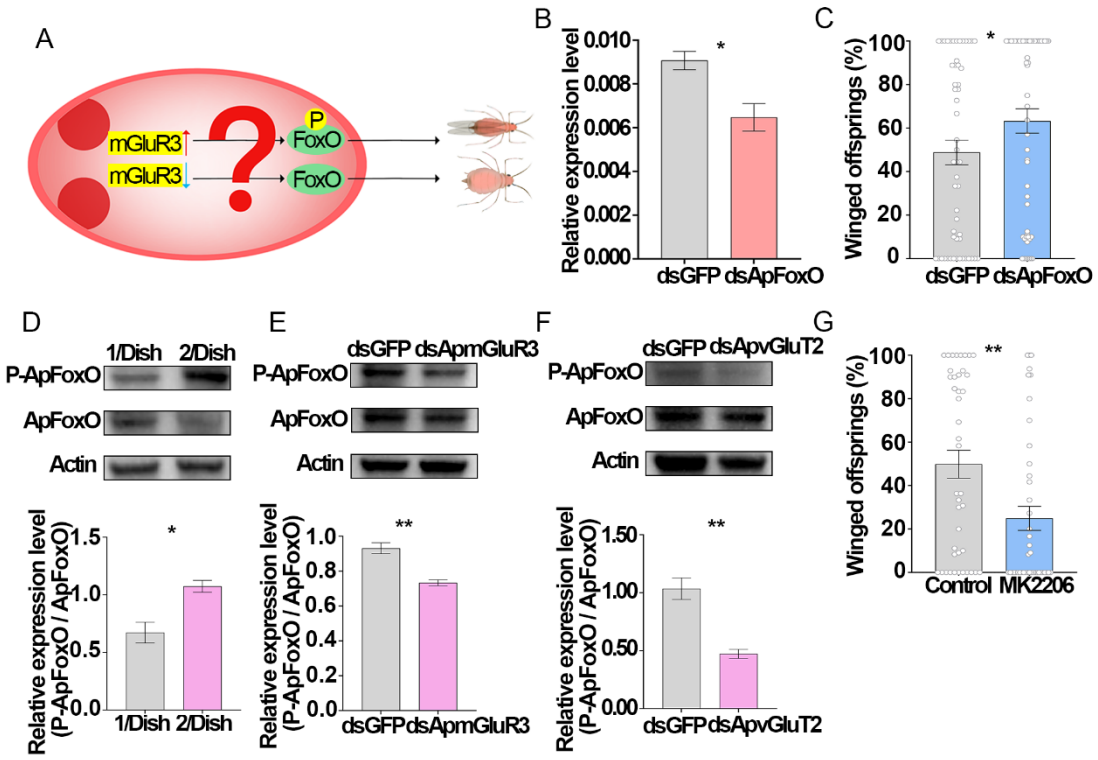


**Figure 4 ApvGluT2 and ApmGluR3 promoted phosphorylation of embryonic ApFoxO, facilitating the formation of winged aphids.** (A) Hypothetical model of *Ap*mGluR3-regulated phosphorylation of *Ap*FoxO in the embryo that controls the wing dimorphism of aphids. (B) RNAi of *ApFoxO* in embryos (n>5), and (C) its effect on the proportion of winged offspring (n>54). (D) The phosphorylated ApFoxO level in the embryo was enhanced by two-adult contacting for 4-hr treatment(n=3) and (E) reduced by ds*ApmGluR3*, and (F) ds*ApvGluT2* (n=3), as determined by western blotting analyses. (G) The proportion of winged offspring was reduced by Akt antagonist MK2206 that directly targeted FoxO as a substrate (n=42). Mann Whitney non-parametric test was used to compare the means of the proportion of winged offspring. Student *t* test was used to compare means of gene transcript or protein level. *P < 0.05, **P < 0.01, ***P < 0.001.

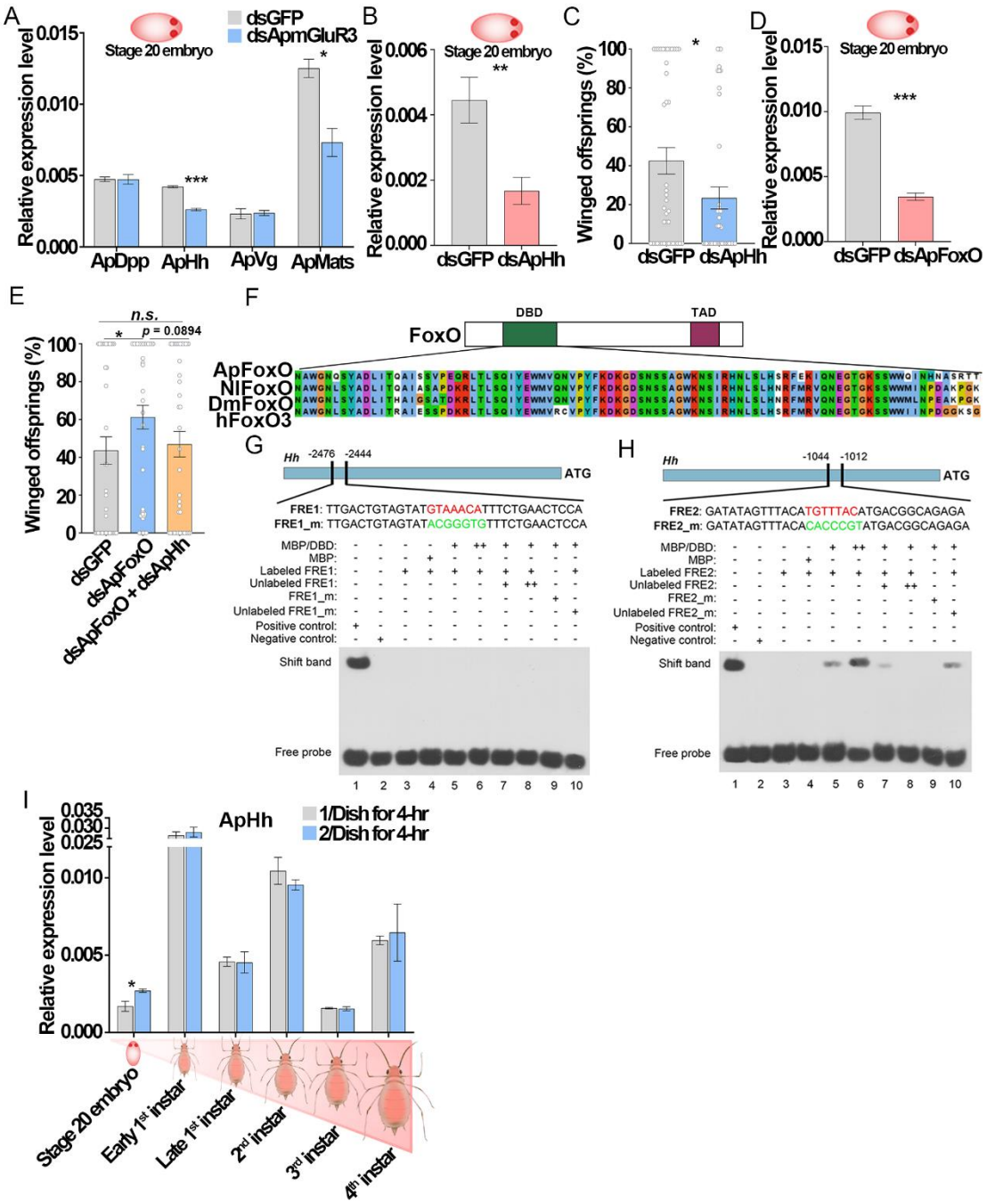


**Figure 5 ApFoxO transcriptionally suppressed *ApHh* at stage 20 embryo.** (A) Knockdown of *ApmGluR3* significantly reduced the transcripts of *hedgehog* (*ApHh*) and *Mob as tumor suppressor* (*ApMats*) in stage 20 embryos (n=3). (B) RNAi efficiency of *ApHh* in stage 20 embryos (n=5). (C) The effects of ds*ApHh* on the proportion of winged offspring (n=42). (D) RNAi efficiency of *ApFoxO* in stage 20 embryos (n=5). (E) The proportion of winged offspring was rescued by knocking down of *ApHh* in

ds*ApFoxO* aphids (n>40). (F) Sequence alignment of DNA binding domains (DBD) among FoxO homologs from brown planthopper (NlFoxO), *Drosophila* (DmFoxO) and human (hFoxO). (G) EMSA showing that Maltose-binding protein (MBP)/ DNA-binding domain (DBD) of ApFoxO fusion failed to bind to *FRE1* (FoxO recognition element 1), but (H) bound to *FRE2* on the *ApHh* promoter. Lane 1: positive control. Lane 2: negative control. Lane 3: biotin-labeled *FRE* only. Lane 4: 0.5 μg recombinant MBP +labeled FRE. Lane 5: 0.5 μg or Lane 6: 5 μg of recombinant MBP/DBD fusion protein + labeled *FRE*. Lane 7: 0.5 μg recombinant MBP/DBD fusion protein + labeled *FRE* + 20 μmol (5 ×) unlabeled *FRE* competitor, or Lane 8: 25 × unlabeled competitor. Lane 9: 0.5 μg recombinant MBP/DBD fusion protein + 5 × biotin-labeled mutant FRE (FRE_m). Lane 10: 0.5 μg recombinant MBP/DBD fusion protein + biotin-labeled FRE + 5 × biotin end-labeled FRE_m. Biotin-labeled *FRE* was all 4 μmol in each lane. (I) Two-adult contacting increased *ApHh* transcripts only at stage 20 embryos relative to solitary aphids (n=5). Mann Whitney non-parametric test was used to compare the means of the proportion of winged offspring. Student *t* test was used to compare means of gene transcript level. *n.s.* not significant, *P < 0.05, **P < 0.01, ***P < 0.001.

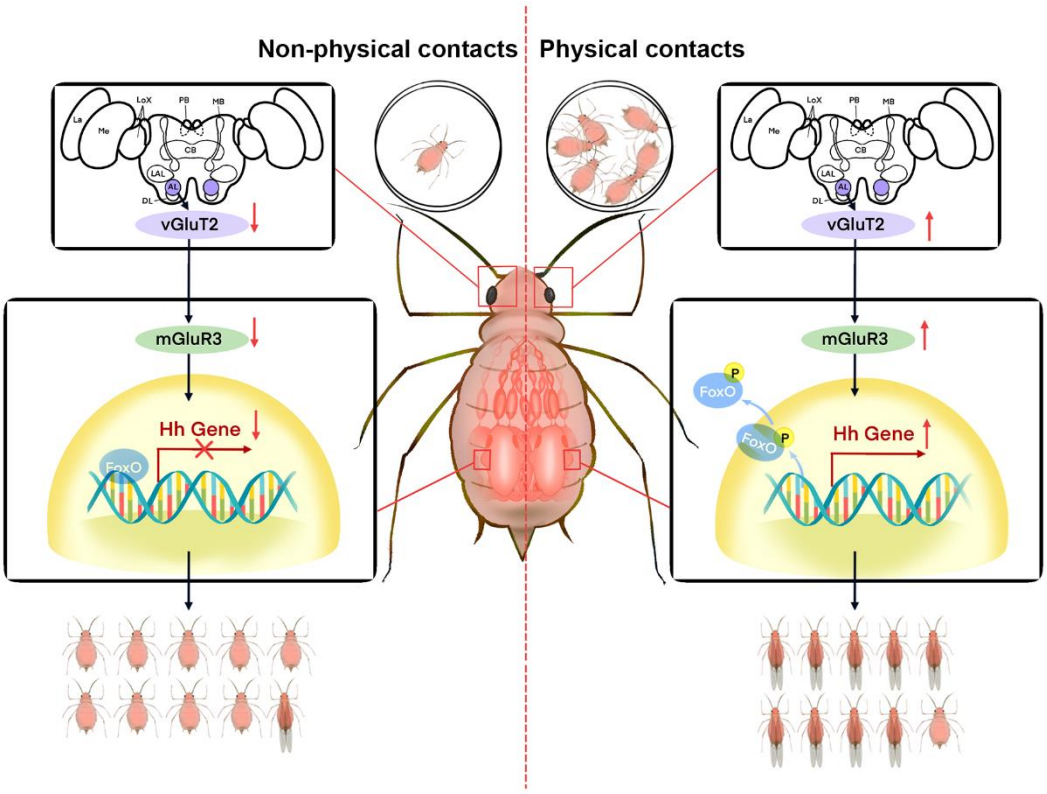


**Figure 6 Illustration of how the ApvGluT2-mGluR3 module transgenerational controls wing morphs in response to physical contact.** In solitary aphids, relatively high level of unphosphorylated ApFoxO binds to the *cis*-element of *ApHh* promoter, suppressing its the expression. of *ApHh* at stage 20 embryo. As a result, the prevalence of wingless offspring was observed. Once experienced physical contact, maternal aphids increased the *ApvGluT2* expression in antennal lobes of the brain and *Ap*m*GluR3* in wing discs of the embryo. This is followed by increased phosphorylation of ApFoxO. The phosphorylated ApFoxO is transported from the nucleus to the cytoplasm, thereby releasing the transcriptional suppression of *ApHh*, leading to high proportion of wingless offspring. vGluT2, vesicular glutamate transporter 2; mGluR3, metabotropic glutamate receptor 3; FoxO, Forkhead transcription factor subgroup O; Hh, hedgehog; La, lamina; Me, medulla; Lox, lobula complex; PB, protocerebral bridge; MB,

767 mushroom body; CB, central body; LAL, lateral accessory lobe; AL, antennal lobe; DL,

768 dolsal lobe.

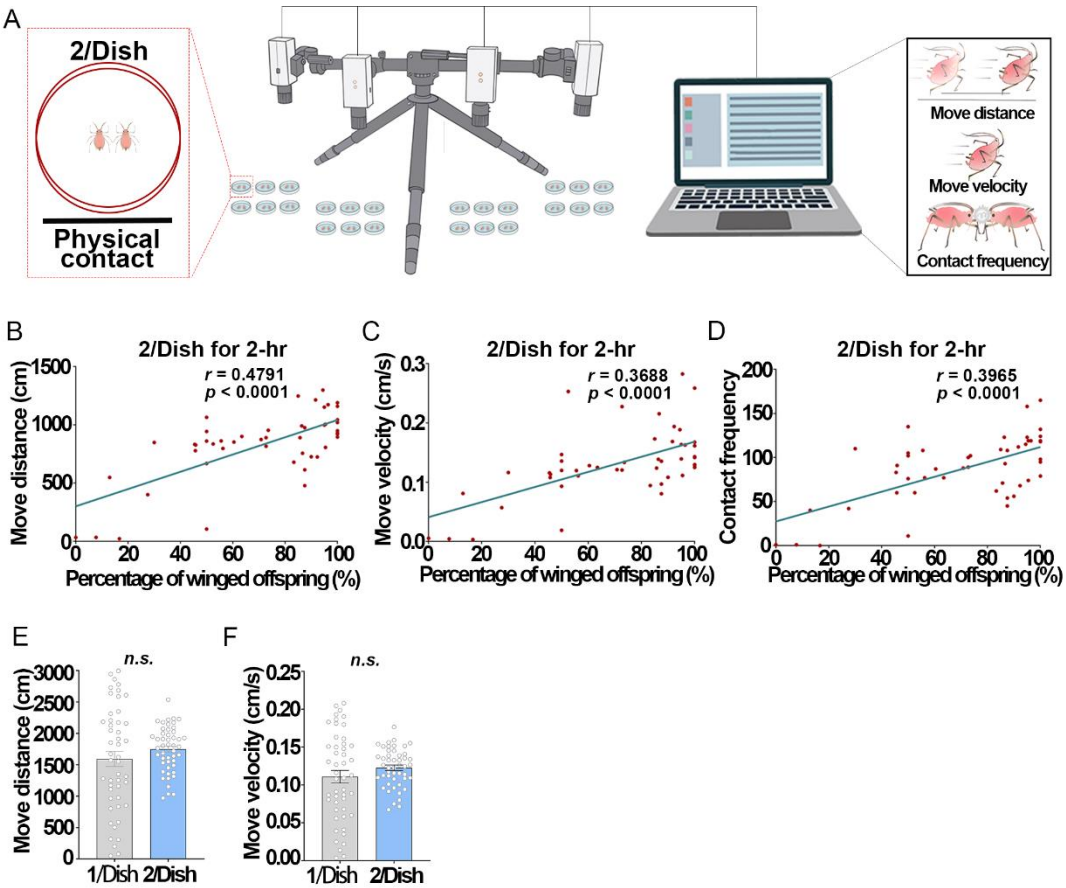


**Figure S1 Correlation between the proportion of winged offspring and maternal locomotor activity.** (A) Schematic diagram of locomotor activity monitoring. (B) Linear regression of the proportion of winged offspring vs the move distance, or (C) the move velocity, or (D) the contact frequency in maternal aphids. (E) The movement distance and (F) velocity of maternal aphids subjected to the two-adult contacting for 4-hr were similar to those of solitary maternal aphids. Student *t* test was used to compare means, n = 48, *n.s.* not significant.

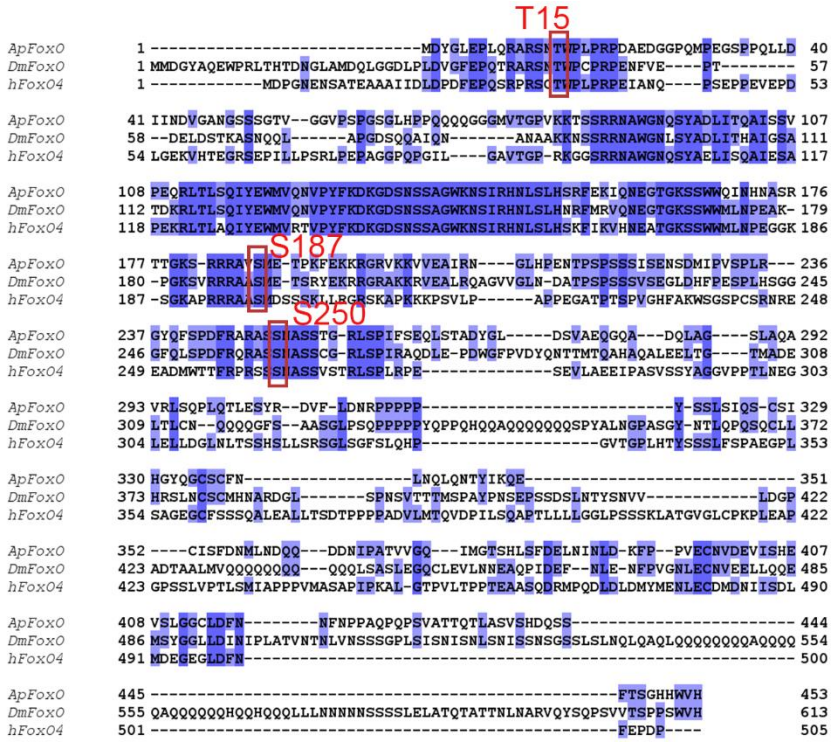


**Figure S2 Multiple amide acid sequence alignment indicating pea aphid FoxO potentially shares three conserved phosphorylation sites with *Drosophila* FoxO and Human FoxO4.** Three conserved phosphorylation sites, including T15, S187 and S250, were highlighted. *Ap*, *Acyrthosiphon pisum*; *Dm*, *Drosophila melanogaster*; *H*, *Homo sapiens*.

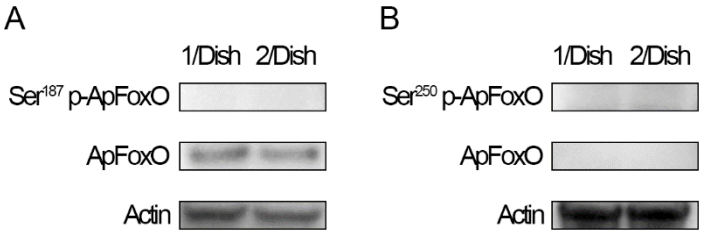


**Figure S3 Evaluation of phosphorylated *Ap*FoxO antibodies used in western blot targeting (A) phosphorylated S187-*Ap*FoxO, and (B) phosphorylated S250-*Ap*FoxO.**

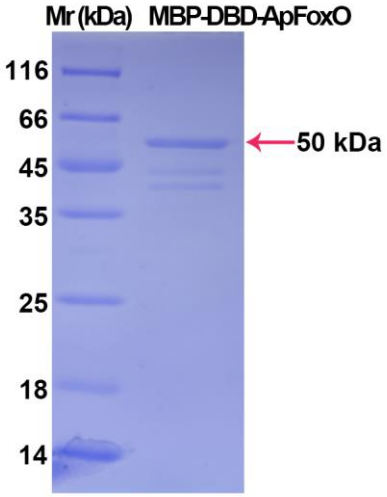


789

790 **Figure S4 SDS-PAGE of purified MBP--DBD$_{ApFoxO}$ recombinant protein.**

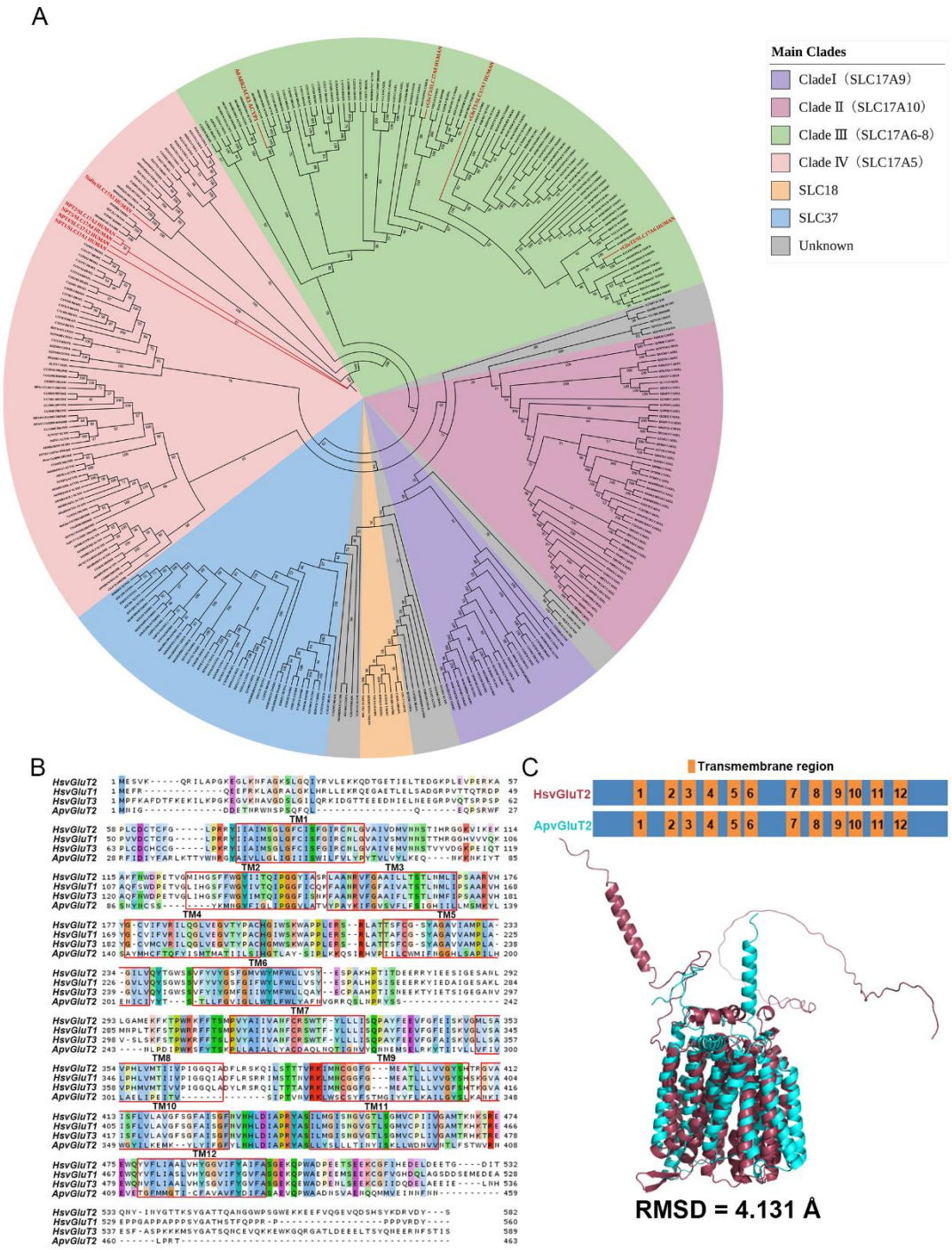


**Figure S5 ApvGluT2 is a structurally conserved protein with 12 transmembrane domains.** (A) The phylogenetic analysis of the vGluT2 family proteins indicated that ApvGluT2 belonged to the Clade III SLC17A9 subfamily. Bootstrap values expressed as percentage of 1000 replications were shown at branch points. Pea aphid vGluT2 (UniProt entry: A0A8R2AC83) and human homologs were highlighted by red

characters. (B) Multiple sequence alignment and (C) pairwise structural alignment indicated that ApvGluT2 containing 12 transmembrane domains were similar to human homologs. Red rectangles marked 12 transmembrane domains. The structure of ApvGluT2 was predicted by AlphaFold2. The pairwise structural alignment was performed by PyMOL software. TM, transmembrane domain. ACYPI, *Acyrthosiphon pisum*; BRAFL, *Branchiostoma floridae*; CAEEL, *Caenorhabditis elegans*; CHICK, *Gallus gallus*; CIOSA, *Ciona savigyni*; DANRE, *Danio rerio*; DROME, *Drosophila melanogaster*; HUMAN, *Homo sapiens*; TAKRU, *Takifugu rubripes*; TETNG, *Tetraodon nigroviridis*. RMSD, root mean square deviation.

## Table S1 Primers for RT-qPCR

| Gene name | Gene ID | Forward | Reverse |
|---|---|---|---|
| RPL27 | ACYPI000085 | 5'–TCGTTACCCTCGGAAAGTC–3' | 5'–GTTGGCATAAGGTGGTTGT–3' |
| vGluT2 | LOC100168565 | 5'–AGGTTTAAGGATCAGCCCGC–3' | 5'–GCCCCAAGATCCCTGGAAAT–3' |
| mGluR3 | LOC107882629 | 5'–CCTCATATTGGACGACTGCGA–3' | 5'–ACGCCTTTCGAAGGTTCTGT–3' |
| GluCl-α | LOC100162577 | 5'–CCATGAACGTTTGGGATGGC–3' | 5'–ATTGGTAACGGCCAGTCTGA–3' |
| Octβ1R | LOC100166522 | 5'–AGTACGCTGTCGTGTCTTCC–3' | 5'–GTGCTTGTTCAGTAACGCGG–3' |
| GLRA1 | LOC100169196 | 5'–GGGTCCAACAAAGTTCACGC–3' | 5'–GGTCCACTGTTCGTCGTCAT–3' |
| HTR2A | LOC100575043 | 5'–GGTCAGACGAGACGGACATC–3' | 5'–GAATCGCCGTGACCCTTTTG–3' |
| FoxO | LOC100168097 | 5'–ACAGTTCGGCTGGATGGAAG–3' | 5'–GGCTCGCGTTGTGGTTTATC–3' |
| Dpp | LOC100163532 | 5'–GTCGGTTGGGACGATTGGAT–3' | 5'–TGGTGGAGTTGAGGTGTTCG–3' |
| Hh | LOC100165590 | 5'–GCGGGAGTGAAGAAGCAGAT–3' | 5'–CACGTTACGGTCCAGGAACA–3' |
| Vg | LOC100570322 | 5'–ACCAACAAGCGTCCACATCT–3' | 5'–CTGCTGTGGTGTGAGTCTGT–3' |
| Mats | LOC100160461 | 5'–CCACTCTTGGTTCGGGCAAT–3' | 5'–CCTCGGTGCAGAACTCTGTT–3' |

## Table S2 Primers for dsRNA synthesis

| Primer name | Gene ID | Forward | Reverse |
|---|---|---|---|
| GFP | - | 5'–CACAAGTTCAGCGTGTCCG–3' | 5'–GTTCACCTTGATGCCGTTC–3' |
| vGluT2 | LOC100168565 | 5'–AGTGCTCCTATCCTCCACGA–3' | 5'–AATATCGCGGGTTCAGGCTC–3' |
| mGluR3 | LOC107882629 | 5'–GTAGTCGAGGGCGATTTGCT–3' | 5'–ACAGATGTGACACTTGACGC–3' |
| FoxO | LOC100168097 | 5'–TTTCTCAGCCGCTACAGACG–3' | 5'–GTCATCCTGCTGGTCGTTCA–3' |